International Journal of Technology (2017) 7: 1266-1275
ISSN 2086-9614

EFFECTS OF THE APPLICATION OF A STERN FOIL ON SHIP RESISTANCE: A CASE STUDY OF AN ORELA CREW BOAT

Ketut Suastika[1*], Affan Hidayat[2], Soegeng Riyadi[2]

[1]*Department of Naval Architecture, Faculty of Marine Technology, Institut Teknologi Sepuluh Nopember (ITS), Jalan Raya ITS, Surabaya 60111, East Java,, Indonesia*
[2]*PT. Orela Shipyard, Jalan Raya Desa Ngemboh RT 02/RW 01, Ujung Pangkah, Gresik 61154, East Java, Indonesia*

(Received: January 2017 / Revised: May 2017 / Accepted: October 2017)

ABSTRACT

The effects of the application of a stern hydrofoil on ship resistance were studied numerically using computational fluid dynamics (CFD) and were verified using data from model tests. A 40 m planing-hull *Orela* crew boat, with target top speed of 28 knots (Froude number, Fr = 0.73), was considered. The stern foil (NACA 64(1)212) was installed with the leading edge positioned precisely below the transom with angle of attack of 2 degrees at elevation 0.853 T below the water surface (where T is the boat's draft). At relatively low speed (Fr < ~0.45) the application of a stern foil results in an increase in ship resistance (of up to 13.9%), while at relatively high speed (Fr > ~0.55) it results in a decrease in ship resistance (of up to 10.0%). As the Froude number increases, the resistance coefficient (C_T) first increases, reaches a maximum value, and then decreases. Its maximum value occurs at $Fr \approx 0.5$, which is consistent with the prediction of a resistance barrier at approximately this Froude number.

Keywords: Computational fluid dynamics (CFD); Planing-hull crew boat; Ship resistance; Stern foil; Towing tests

1. INTRODUCTION

In ship design, one of the key optimization variables is the minimization of ship resistance, which can be achieved through an optimal hull-form design (Campana et al., 2017; Diez et al., 2017; Suastika et al., 2017) or by the application of devices such as bulbous bows, trim wedges, interceptors, or more recently the Hull Vane® (Uithof et al., 2016; Uithof et al., 2017). The focus of the present study is on the application of a stern foil (the Hull Vane®) as a resistance-reduction device (or fuel-saving device).

The Hull Vane® is a submerged hydrofoil installed below the transom (on the stern) of a ship which will generate dynamic lift and additional thrust when the ship moves in water, thereby affecting the ship's trim and wetted surface area (WSA). At relatively high speed, it can result in a net reduction of the ship's total resistance. The Hull Vane® was invented by van Oossanen in 1992 and patented in 2002. It has been successfully applied to many vessels, including a 55 m fast supply intervention vessel, *MV Karina*, and a 42 m superyacht, *Alive* (Bouckaert et al., 2016).

The principle of the Hull Vane® and its effects, which can lead to a resistance reduction (fuel saving), are described by Bouckaert et al. (2015) and Uithof et al. (2017). The lift-force

*Corresponding author's email: k_suastika@na.its.ac.id, Tel: +62-31-594-7254, Fax: +62-31-596-4182
Permalink/DOI: https://doi.org/10.14716/ijtech.v8i7.691

generated by the Hull Vane® can be decomposed into a force in a forward longitudinal-direction (reducing the resistance of the vessel) and in a vertical direction (influencing the trim) in order to reduce the total ship resistance. Additionally, the Hull Vane® reduces the generation of waves and the vessel's motions in waves (reducing added wave resistance). Resistance reductions of up to 26.5% have been found to result from the use of the Hull Vane®, as emerged from CFD computations, model tests and sea trials. For commercial applications, resistance reductions of between 5% and 10% are common. The Hull Vane® is especially applicable on ships sailing at moderate to high non-planing speeds, with Froude numbers between 0.2 and 0.7.

Utilizing CFD computations, Uithof et al. (2016) compared the influence of the Hull Vane®, interceptors, trim wedges, and ballasting on the performance of the 50 m AMECRC series #13 patrol vessel. They demonstrated that the Hull Vane® achieved the highest resistance reduction over the major part of the speed range, with reductions of up to 32.4%. The influence of the different trim-correction devices on the vessel's performance in waves was also assessed. It was found that the Hull Vane® effectively reduced the pitching motion and the added resistance in waves to a greater extent than, for example, an interceptor. Furthermore, Bouckaert et al. (2015, 2016) reported a reduction in total fuel consumption of 12.5% when the Hull Vane® was installed and a small modification to the ship's hull was made. When traveling at the speed at which most fuel was consumed (17.5 knots), the total resistance was reduced by 15.3%.

The achievements of the patented Hull Vane® in reducing ship resistance (thus reducing fuel consumption) have been reported previously (Bouckaert et al., 2015, 2016; Uithof et al., 2016, 2017). The purpose of the present study is to investigate whether such a resistance reduction can be achieved by employing commonly-used foil types, such as those from the NACA series (Abbott & von Doenhoff, 1959). In addition, the foil itself (and the struts) will generate drag, which can increase the total ship resistance, particularly at relatively low speed. Previous research has not sufficiently ascertained within which range of Froude numbers such an increase in resistance will take place. The present results can supplement the previous findings and enrich the literature on the application of a stern foil as a fuel-saving device.

2. METHODS

To study the stern foil's effects on ship resistance, CFD computations were carried out and the results were verified using data from model tests. A 40 m planing-hull *Orela* crew boat was considered with a target top speed of 28 knots (Froude number, Fr = 0.73). The principal dimensions of the boat are summarized in Table 1.

Table 1 Principal dimensions of the *Orela* crew boat

Length overall (L_{oa})	40.00 m
Length between perpendiculars (L_{pp})	39.90 m
Breadth (B)	8.00 m
Height (H)	4.40 m
Draft (T)	1.70 m
Target top speed (V_s)	28 kn
Displacement (Δ)	242.72 t

The CFD computations utilize the Reynolds-averaged Navier-Stokes method to solve the viscous flow field. The mass and momentum equations are given in Equations 1 and 2, respectively.

$$\frac{\partial \rho}{\partial t} + \frac{\partial}{\partial x_i}(\rho u_i) = 0 \quad (1)$$

$$\frac{\partial}{\partial t}(\rho u_i) + \frac{\partial}{\partial x_j}(\rho u_i u_j) = -\frac{\partial p}{\partial x_i} + \frac{\partial}{\partial x_j}\left[\mu\left(\frac{\partial u_i}{\partial x_j} + \frac{\partial u_j}{\partial x_i} - \frac{2}{3}\delta_{ij}\frac{\partial u_l}{\partial x_l}\right)\right] + \frac{\partial}{\partial x_j}\left(-\rho\overline{u'_i u'_j}\right) \quad (2)$$

where $-\rho\overline{u'_i u'_j}$ are the Reynolds stresses, which must be modeled to close Equation 2.

The turbulence model used in the present study is the SST *k-ω* model (Menter, 1994), which gives accurate predictions of the onset and the amount of flow separation (Bardina et al., 1997). This is a combination of the *k-ω* model for the flow in the inner boundary layer and the *k-ε* model for the flow in the outer region of and outside of the boundary layer. The transport equations for the SST *k-ω* model are as follows:

$$\frac{\partial}{\partial t}(\rho k) + \frac{\partial}{\partial x_i}(\rho k u_i) = \frac{\partial}{\partial x_j}\left(\Gamma_k \frac{\partial k}{\partial x_j}\right) + G_k - Y_k \quad (3)$$

$$\frac{\partial}{\partial t}(\rho \omega) + \frac{\partial}{\partial x_i}(\rho \omega u_i) = \frac{\partial}{\partial x_j}\left(\Gamma_\omega \frac{\partial \omega}{\partial x_j}\right) + G_\omega - Y_\omega + D_\omega \quad (4)$$

In Equations 3 and 4, G_k represents the generation of turbulence kinetic energy due to mean velocity gradients, while G_ω represents the generation of ω. Y_k and Y_ω represent the dissipation of k and ω due to turbulence, respectively. Γ_k and Γ_ω represent the effective diffusivity of k and ω, respectively, while D_ω represents the cross-diffusion term.

More recently, Ramdlan et al. (2016) compared different turbulence models (namely, STD k-ε, RNG k-ε, and the Reynolds stress model, RSM) by analyzing the nature or characteristics of flow in a wind tunnel utilizing CFD simulations, and found that the RSM gave the best results.

In the following sections, CFD simulations of the foil alone and of the ship with and without foil are further elaborated to determine an optimum foil size and to study the foil's effects on ship resistance.

2.1. CFD Simulations of the Foil Alone

Simulations of the foil alone were undertaken to determine the optimum foil size and to analyze the foil's lift-to-drag ratio with varying angles of attack (α). Two foil types from the NACA series were investigated, namely, NACA 64(1)212 and NACA 21021 (Abbott & von Doenhoff, 1959). Figure 1 shows a mesh of the NACA 64(1)212 foil, while Figure 2 shows the position of the foil in the computational domain.

In the simulations, the foil's span was kept constant, equal to the breadth of the ship, but the chord length was varied. Furthermore, the foil's aspect ratio was kept within the recommended range (van Walree, 1999).

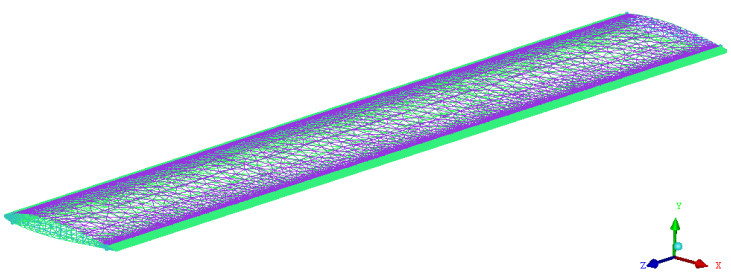

Figure 1 Mesh of the NACA 64(1)212 foil

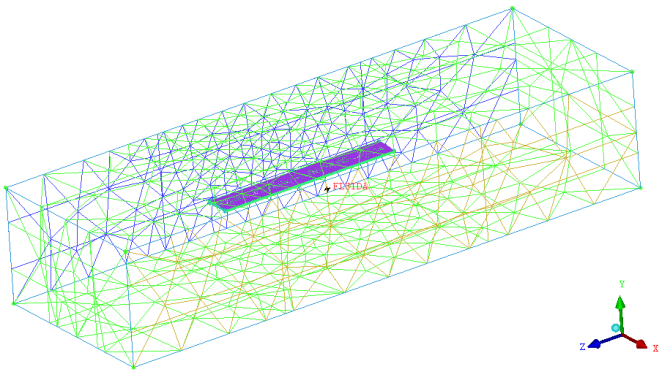

Figure 2 Position of the foil in the computational domain

The boundary conditions of the computational domain are as follows (Versteeg & Malalasekera, 2007). The inlet boundary, located at 1-*c* upstream from the leading edge (where *c* is the chord length), is defined as a uniform flow with velocity equaling the ship/foil's velocity. (In the simulations, the foil is at rest, but the water flows.) In the outlet boundary, at a location 4-*c* downstream from the trailing edge, the pressure equals the undisturbed (hydrostatic) pressure, ensuring no upstream propagation of disturbances (Mitchel et al., 2008). The boundary condition on the foil's surface is defined as no-slip condition. The boundary conditions on the top and bottom walls (at a distance of 2-*c* above and below the foil, respectively), and on the side walls (approximately 7-*c* away from the side of the model) are defined as free-slip condition. Furthermore, because the foil is fully submerged at a relatively deep submergence elevation (the foil's thickness is much smaller than the submerged depth), and in order to reduce the time of convergence, free surface effects (generation of waves) were not modeled in this case.

To determine the optimum grid size (number of elements), tests were carried out such that the numerical solution fulfills the grid-independence criterion (Anderson, 1995). The root mean square (rms) error criterion with a residual target value of 10^{-5} was used as the criterion for the convergence of the numerical solutions.

2.2. CFD Simulations of the Ship with and without Foil

Simulations of the ship with and without stern foil were undertaken to study the effects of the stern foil on ship resistance. Free surface effects (generation of waves) were modeled in this case, for which the volume of fluid method was utilized (Hirt & Nichols, 1981). The transport equation for a volume fraction (φ) in the absence of diffusion and source/sink terms is represented as follows:

$$\frac{\partial \varphi}{\partial t} + \frac{\partial}{\partial x_i}(\varphi u_i) = 0 \tag{5}$$

Two boundary conditions have to be fulfilled at the free surface, namely, the kinematic and dynamic boundary conditions (see, for example, Vaz et al., 2009). The kinematic boundary condition states that the free surface is a material surface, while the dynamic boundary condition states that the pressure at the free surface is equal to the atmospheric pressure.

The remaining boundary conditions of the computational domain are as follows (Versteeg & Malalasekera, 2007). The inlet boundary, located at 1-*L* upstream from the ship (where *L* is the ship's length at the water line), is defined as a uniform flow with velocity equaling the ship's velocity. (In the simulations, the ship is at rest, but the water flows.) The outlet boundary, at a

location 4-*L* downstream from the ship, is also given as a uniform flow with velocity equaling that of the ship. The boundary conditions on the surface of the ship's hull, foil and struts are defined as no-slip condition. Meanwhile, the boundary conditions on the bottom wall, at approximately 1-*L* below the mean water surface, and on the top wall, at approximately 0.2-*L* above the mean water surface, are defined as free-slip condition. The boundary conditions on the side walls (0.4-*L* away from the side of the model) are defined as symmetric pressure condition. This means that the pressure inside the wall is equal to the pressure outside the wall; there is no wave-reflection due to the side walls.

The stern foil was mounted transversally and parallel to the water surface using two struts with the leading edge placed precisely below the transom at elevation 0.853 *T* below the water surface (see Figure 3; the submerged elevation of the foil is h_f = 1.45 m below the water surface; the draft is T = 1.70 m; h_f/T = 1.45/1.70 = 0.853). The struts are symmetrical foils, which are NACA 0010 with chord length of 1.2 m (the same length as that of the stern foil).

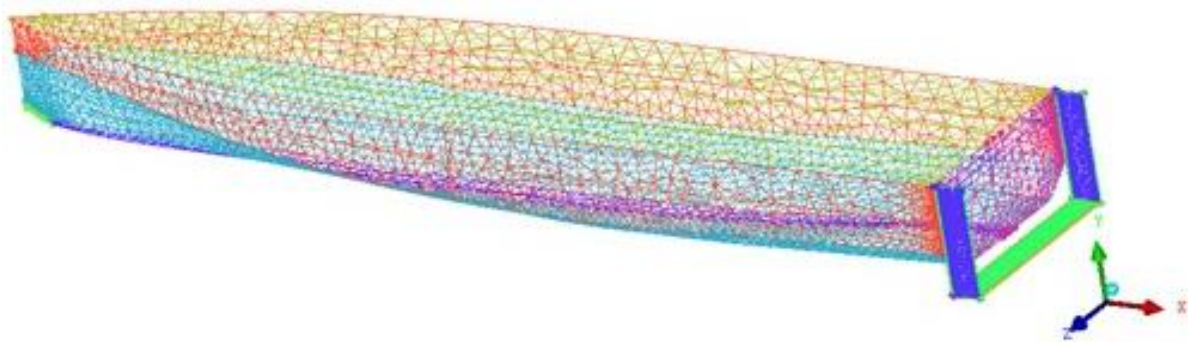

Figure 3 Mesh of the ship's hull with the stern foil attached using two struts

To determine the optimum grid size (number of elements), tests were carried out such that the numerical results complied with the grid-independence criterion (Anderson, 1995). The rms error criterion with a residual target value of 10^{-4} was used as the criterion for the convergence of the numerical solutions.

2.3. Towing-tank Experiments

To verify the results of the CFD simulations, experiments were conducted in the towing tank of the Hydrodynamic Laboratory of the Faculty of Marine Technology, ITS Surabaya, Indonesia. The dimensions of the towing tank are as follows: length = 50.0 m, width = 3.0 m, and water depth = 2.0 m.

Models were designed and manufactured for the ship hull, the stern foil and the struts with a (geometrical) scale of 1:40. The ship model was made from fiberglass-reinforced plastic, which was coated with paint and resin. The stern hydrofoil (NACA 64(1)212) was made from brass, while the struts (NACA 0010) were made from mica. Figures 4a and 4b show the side and aft views, respectively, of the ship model with the stern foil attached to the hull using two struts.

The model's resistance was measured by using a load cell. The load cell was connected to a voltage amplifier, which was in turn connected to a computer network in the control room. Before carrying out a measurement, the load cell was calibrated by using a mass of 1.0 kg. Six ship speeds were tested: 1.14, 1.30, 1.46, 1.63, 1.79 and 1.95 m/s (full-scale speeds: 14, 16, 20, 22, 24 knots). Figure 5 shows a photograph of the model being towed at a speed of 1.46 m/s (full-scale speed: 20 knots; Fr = 0.52).

(a) Side view

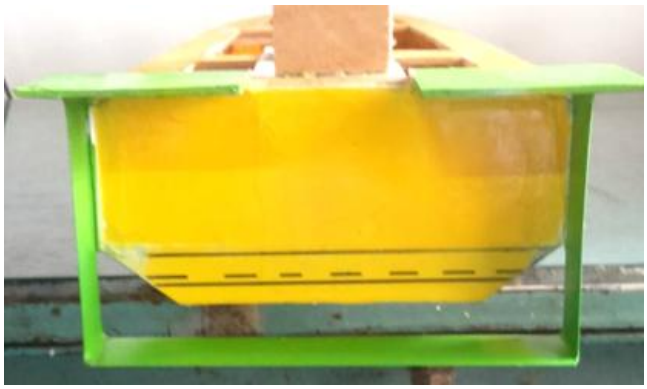

(b) Aft view

Figure 4 Ship model with the stern foil attached to the hull using two struts (scale 1:40)

Figure 5 Ship model towed at a speed of 1.46 m/s (full-scale speed = 20 knots; Froude number Fr = 0.52)

3. RESULTS AND DISCUSSION

Table 2 summarizes the effect of different foil aspect ratios on the lift-to-drag ratio as obtained from simulations of the foil alone with angle of attack α = 0°. The results show that, for the same foil size (aspect ratio), the NACA 64(1)212 foil has a greater lift-to-drag ratio than the NACA 21021 foil. Furthermore, the lift-to-drag ratio increases with increasing aspect ratio (for both the cases considered). The NACA 64(1)212 foil with an aspect ratio of 6.67 has the greatest lift-to-drag ratio. Therefore, it was chosen as the stern foil of the *Orela* crew boat.

Table 2 Lift-to-drag ratio C_L/C_D for the NACA 64(1)212 and NACA 21021 foils with angle of attack $\alpha = 0°$ and different foil aspect ratios

Chord (m)	Span (m)	Aspect ratio	C_L/C_D	
			NACA 64(1)212	NACA 21021
1.20	8.00	6.67	18.70	5.84
1.60	8.00	5.00	15.94	5.25
2.00	8.00	4.00	13.98	3.49

Figure 6 shows the lift-to-drag ratio for the NACA 64(1)212 foil with an aspect ratio of 6.67 as a function of angle of attack (α). The value of C_L/C_D first increases, takes a maximum value, and then decreases monotonically with increasing angle of attack. The maximum value of C_L/C_D is approximately 30.0 which is reached at $\alpha \approx 2°$ (stall). Therefore, in the simulations of the ship with the stern foil, the foil's angle of attack was set at $\alpha = 2°$.

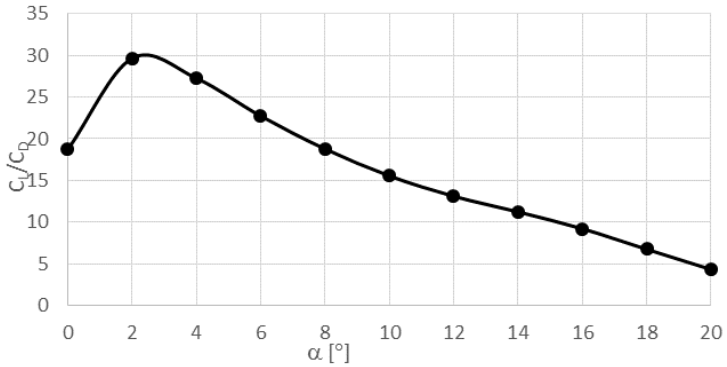

Figure 6 Lift-to-drag ratio of the NACA 64(1)212 foil with an aspect ratio of 6.67 as a function of angle of attack (α)

Figure 7 shows the total ship resistance (R_T) as a function of the Froude number (Fr) obtained from CFD simulations, experiments, and the Holtrop-Mennen-Savitsky model (Holtrop & Mennen, 1982; Savitsky, 1964). The results demonstrate that at relatively low speed (Fr < ~0.45) the stern foil results in an increase in the total ship resistance. For example, at Fr = 0.36 and 0.42 (ship speed = 14 and 16 knots), the total resistances of the ship with the stern foil are, respectively, 13.9% and 11.8% greater than those without the stern foil. On the other hand, at relatively high speed (Fr > ~0.55) the stern foil results in a decrease in the total ship resistance. At Fr = 0.57, 0.62 and 0.73 (ship speed = 22, 24 and 28 knots), for example, the total ship resistance decreases by 8.4%, 7.1% and 10.0%, respectively.

Utilizing the Hull Vane® with varying positions and considering a 50 m offshore patrol vessel, Bouckaert et al. (2016) reported a decrease in resistance (of up to 23%) in the range of Fr > ~0.21. Uithof et al. (2017) applied the Hull Vane® to 42 m, 47 m, and 55 m motor yachts and to a 300 m container vessel, and also reported a decrease in resistance (of up to 30%) for Fr > ~0.21. Clearly, the resistance reduction depends on the vessel under consideration and the type of foil applied. The above results show that the performance of the Hull Vane® is generally better than the performance of the NACA 64(1)212 foil when applied to a planing-hull crew boat, as considered in the present study.

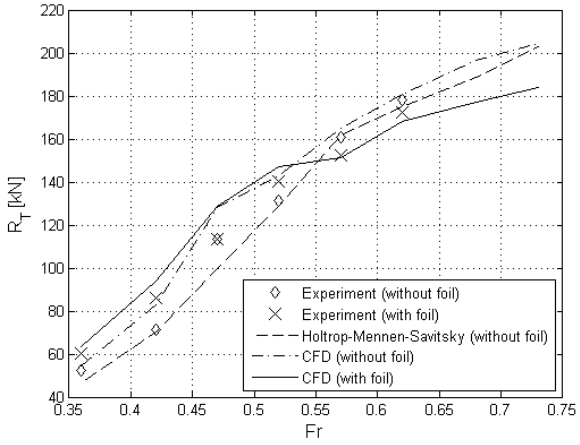

Figure 7 Total ship resistance (R_T) as a function of the Froude number (Fr)

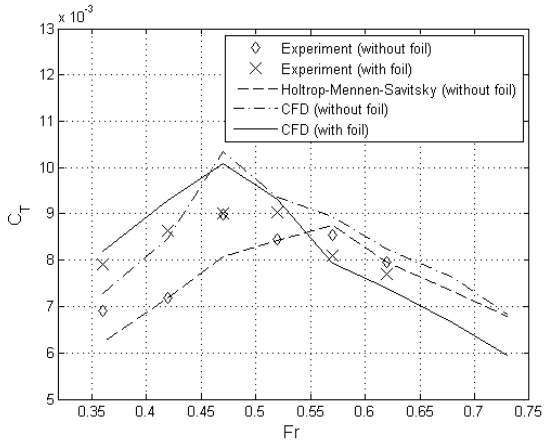

Figure 8 Coefficient of the total ship resistance (C_T) as a function of the Froude number (Fr)

In addition to Figure 7, Figure 8 shows plots of the total resistance coefficient (C_T) as a function of the Froude number (Fr). The resistance coefficient is calculated as

$$C_T = \frac{R_T}{\frac{1}{2}\rho V^2 A} \tag{6}$$

where R_T is the total ship resistance, ρ is the mass density of water, V is the ship speed, and A is the WSA. The results demonstrate that, as the Froude number increases, the resistance coefficient first increases, takes a maximum value, and then decreases. The maximum value of C_T, the so-called resistance barrier, is observed at $Fr \approx 0.47$. Earlier studies (Marshall, 2002; Yousefi et al., 2013) predict the resistance barrier to occur at $Fr \approx 0.5$, which is in good agreement with the present finding.

Comparing the values of C_T for the cases with and without the stern foil, it can be seen that, at relatively low speed (Fr < ~0.45), the stern foil increases the resistance coefficient, but at relatively high speed (Fr > ~0.55), it causes a decrease in the resistance coefficient. For the case without foil, the CFD results generally overestimate the experimental data. Furthermore, the Holtrop-Mennen-Savitsky model (Holtrop & Mennen, 1982; Savitsky, 1964) provides a good prediction for the total resistance coefficient, but it underestimates the value of C_T at the resistance barrier ($Fr \approx 0.47$). For the case with the stern foil, the CFD results overestimate the experimental data at relatively low Froude numbers, but slightly underestimate the experimental data at relatively high Froude numbers.

4. CONCLUSION

A 40 m planing-hull *Orela* crew boat was considered in a study utilizing computational fluid dynamics (CFD) and towing-tank experiments to investigate the effects of the application of a stern foil on ship resistance. At relatively low speed (Froude number Fr < ~0.45), the stern foil results in an increase in ship resistance (of up to 13.9%), while at relatively high speed (Fr > ~0.55), it results in a decrease in ship resistance (of up to 10.0%). The above results are consistent with the results of previous research utilizing the Hull Vane®, though the Hull Vane® exhibits a better performance (Bouckaert et al., 2016; Uithof et al., 2017). The resistance barrier is observed to occur at $Fr \approx 0.47$, which is in good agreement with the prediction of previous studies (Marshall, 2002; Yousefi et al., 2013). For the case without a foil, the Holtrop-Mennen-Savitsky model (Holtrop and Mennen, 1982; Savitsky, 1964) provides a good prediction for the

total resistance coefficient (C_T), but it underestimates the value of C_T at the resistance barrier ($Fr \approx 0.47$).

5. ACKNOWLEDGEMENT

This research project was financially supported by the Indonesian Ministry of Research, Technology and Higher Education (RISTEKDIKTI), under the grant: *Penelitian Kerjasama Industri* 2017 with contract no. 562/PKS/ITS/2017.

6. REFERENCES

Abbott, I.H., von Doenhoff, A.E., 1959. *Theory of Wing Sections (Including a Summary of Airfoil Data).* New York: Dover Publications, Inc.

Anderson Jr., J.D., 1995. *Computational Fluid Dynamics: The Basics with Applications*. New York: McGraw-Hill, Inc.

Bardina, J.E., Huang, P.G., Coakley, T.J., 1997. *Turbulence Modeling Validation, Testing, and Development*. NASA Technical Memorandum 110446, Ames Research Center, Moffett Field, California, USA

Bouckaert, B., Uithof, K., van Oossanen, P., Moerke, N., Nienhuis, B., van Bergen, J., 2015. A Life-cycle Cost Analysis of the Application of a Hull Vane® to an Offshore Patrol Vessel. *In*: Proceeding of the 13th International Conference on Fast Sea Transport (FAST), Washington DC, USA

Bouckaert, B., Uithof, K., Moerke, N., van Oossanen, P.G., 2016. Hull Vane® on 108-m Holland-Class OPVs: Effects on Fuel Consumption and Seakeeping. *In*: Proceeding of MAST Conference 2016, Amsterdam, Netherlands

Campana, E.F., Diez, M., Liuzzi, G., Lucidi, S., Pellegrini, R., Piccialli, V., Rinaldi, F., Serani, A., 2017. A Multi-objective DIRECT Algorithm for Ship Hull Optimization. *Computational Optimization and Applications*, Volume 68(195), https://doi.org/10.1007/s10589-017-9955-0.

Diez, M., Serani, A., Campana, E.F., Stern, F., 2017. CFD-based Stochastic Optimization of a Destroyer Hull Form for Realistic Ocean Operations. *In*: Proceeding of the 14th International Conference on Fast Sea Transportation (FAST 2017), Nantes, France

Hirt, C.W., Nichols, B.D., 1981. Volume of Fluid (VoF) Method for the Dynamics of Free Boundaries. *Journal of Computational Physics*, Volume 39(1), pp. 201–225

Holtrop, J., Mennen, G.G.J., 1982. An Approximate Power Prediction Method. *International Shipbuilding Progress*, Volume 29(335), pp. 166–170

Marshall, R., 2002. *All About Powerboats: Understanding Design and Performance*. New York: McGraw-Hill Professional

Menter, F.R., 1994. Two-equation Eddy-viscosity Turbulence Models for Engineering Applications. *AIAA Journal*, Volume 32(8), pp. 1598–1605

Mitchel, R.R., Webb, M.B., Roetzel, J.N., Lu, F.K., Dutton, J.C., 2008. A Study of the Base Pressure Distribution of a Slender Body of Square Cross Section. *In*: Proceeding of the 46th AIAA Aerospace Sciences Meeting and Exhibition, Reno, Nevada, pp. 1–8

Ramdlan, G.G., Siswantara, A.I., Budiarso, B., Daryus, A., Pujowidodo, H., 2016. Turbulence Model and Validation of Air Flow in Wind Tunnel. *International Journal of Technology*, Volume 7(8), pp. 1362–1372

Savitsky, D., 1964. Hydrodynamic Design of Planing Hulls. *Marine Technology*, Volume 1(1), pp. 71–95

Suastika, K., Nugraha, F., Utama, I.K.A.P., 2017. Parallel-middle-body and Stern-form Relative Significance in the Wake Formation of Single-screw Large Ships. *International Journal of Technology*, Volume 8(1), pp. 94–103

Uithof, K., Hagemeister, N., Bouckaert, B., van Oossanen, P.G., Moerke, N., 2016. A Systematic Comparison of the Influence of the Hull Vane®, Interceptors, Trim Wedges, and Ballasting on the Performace of the 50-m AMECRC Series #13 Patrol Vessel. *In*: Warship 2016: Advanced Technologies in Naval Design, Construction, & Operation, 15-16 June 2016, Bath, UK

Uithof, K., van Oossanen, P., Moerke, N., van Oossanen, P.G., Zaaijer, K.S., 2017. *An Update on the Development of the Hull Vane®*. Available online at www. hullvane.nl, Accessed on March 27, 2017

van Walree, F., 1999. Computational Methods for Hydrofoil Craft in Steady and Unsteady Flow. *Ph.D. Thesis*, Delft University of Technology, Netherlands

Vaz, G., Jaouen, F., Hoekstra, M., 2009. Free-surface Viscous Flow Computations. Validation of URANS Code FRESCO. *In*: ASME 28th International Conference on Ocean, Offshore and Arctic Engineering (OMAE 2009), May 31-June 5, 2009, Honolulu, Hawaii

Versteeg, H.K., Malalasekera, W., 2007. *An Introduction to Computational Fluid Dynamics: The Finite Volume Method*. Harlow, UK: Longman Scientific

Yousefi, R., Shafaghat, R., Shakeri, M., 2013. Hydrodynamic Analysis Techniques for High-speed Planing Hulls. *Applied Ocean Research*, Volume 42, pp. 105–113